

# Compressible Flows inside Piston Ring Pack Simulated with Space-Time Finite Elements

Max von Danwitz<sup>1\*</sup>, Norbert Hosters<sup>1</sup> and Marek Behr<sup>1</sup>

## Micro Abstract

The fuel efficiency of an internal combustion engine is directly related to the performance of the piston ring pack. We present our numerical study of compressible gas flow in the ring pack. Namely, a two-dimensional transient full engine working cycle simulation considering the fluid-rigid-body interaction between piston ring and surrounding fluid, and a three-dimensional simulation of the flow through the ring gap investigating the gap's suction effect.

<sup>1</sup>Chair for Computational Analysis of Technical Systems, RWTH Aachen University, Aachen, Germany

\*Corresponding author: Danwitz@cats.rwth-aachen.de

## Introduction

The pistons of an internal combustion engine are equipped with the piston ring pack to seal the combustion chamber and minimize leakage gas flow to the crank case. During the working cycle of the engine, the rings (Figure 1a) slide along the encompassing cylinder wall (liner). The resulting friction contributes significantly to the frictional losses of the engine [1].

Hence, an alternative design of the piston rings, which reduces the friction between piston and liner, but, only moderately increases the gas flow around the piston rings (blow-by), can improve the overall efficiency of the engine. To find such a design, detailed knowledge about the fluid flow in the piston ring pack is necessary. As experimental and theoretical studies are difficult to conduct [2], we propose a numerical approach in this contribution.

## 1 Numerical Methodology

To model the gas flow, we employ the compressible Navier-Stokes equations based on conservation of mass, momentum, and energy. We follow [5], in choosing the pressure-primitive variables  $\mathbf{Y}$

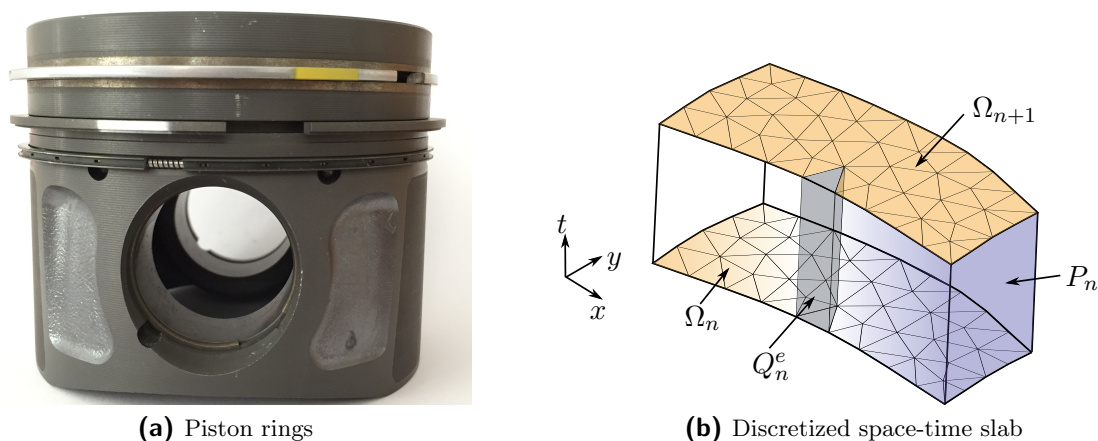


Figure 1. Physical and computational geometry

as primary unknowns in contrast to the more commonly used conservation variables  $\mathbf{U}$ :

$$\mathbf{Y} = [p, u_1, u_2, u_3, T]^\top, \quad \mathbf{U} = [\rho, \rho u_1, \rho u_2, \rho u_3, \rho e_{tot}]^\top. \quad (1)$$

An advantage of this choice is that pressure and temperature can be directly incorporated into the model as essential boundary conditions. As in [5], a reduced form of the energy equation is used in deriving a quasi-linear form:

$$\mathbf{Res}(\mathbf{Y}) = \mathbf{A}_0 \mathbf{Y}_{,t} + (\mathbf{A}_i^a + \mathbf{A}_i^p) \mathbf{Y}_{,i} - (\mathbf{K}_{ij} \mathbf{Y}_{,j})_{,i} = \mathbf{0}, \quad \mathbf{A}_0 = \frac{\partial \mathbf{U}}{\partial \mathbf{Y}}. \quad (2)$$

For the definition of the generalized advective-diffusive system matrices  $\mathbf{A}_i$ , and  $\mathbf{K}_{ij}$ , we refer to [5]. The quasi-linear form is transformed into a weak form and discretized using equal order space-time finite elements.

$$\begin{aligned} & \int_{Q_n} \mathbf{W} \cdot (\mathbf{A}_0 \mathbf{Y}_{,t} + \mathbf{A}_i^a \mathbf{Y}_{,i}) dQ + \int_{Q_n} \mathbf{W}_{,i} \cdot (\mathbf{K}_{ij} \mathbf{Y}_{,j} - \mathbf{A}_i^p \mathbf{Y}) dQ - \int_{(P_n)_h} \mathbf{W} \cdot \mathbf{h} dP \\ & + \sum_{e=1}^{(n_{el})_n} \int_{Q_n^e} \boldsymbol{\tau}^e ((\mathbf{A}_i)^T \mathbf{W}_{,i}) \cdot \mathbf{Res}(\mathbf{Y}) dQ + \int_{\Omega_n} (\mathbf{W})_n^+ \cdot \mathbf{A}_0 ((\mathbf{Y})_n^+ - (\mathbf{Y})_n^-) d\Omega = \mathbf{0}. \end{aligned} \quad (3)$$

The first three terms, are the quasi-linear form multiplied with the test function vector  $\mathbf{W}$ . The pressure contribution to the advection  $\mathbf{A}_i^p \mathbf{Y}$  and the diffusive term  $\mathbf{K}_{ij} \mathbf{Y}_{,j}$  are integrated by parts leading to the integral over the Neumann boundary  $(P_n)_h$ . An exemplary space-time slab  $Q_n$  with the used integration domains can be seen in Figure 1b. To ensure numerical stability, an SUPG stabilization operator is added to the weak form (fourth term). The stabilization matrix  $\boldsymbol{\tau}^e$  is defined as in [5] using the element metric tensor  $\mathbf{G}$  as an representation of the element length. To prevent an influence of the nodal ordering for triangular or tetrahedral elements, the mapping  $\mathbf{K}$  of the reference element to an equilateral element is included [3]:

$$\boldsymbol{\tau}^e = \mathbf{A}_0^{-1} \left( \frac{4}{\Delta t^2} \mathbf{I} + \mathbf{G}_{ij} \mathbf{A}_i \mathbf{A}_j + \frac{1}{C_M^2} \mathbf{G}_{ij} \mathbf{G}_{kl} \mathbf{K}_{ik} \mathbf{K}_{lj} \right)^{-\frac{1}{2}}, \quad \mathbf{G} = \left( \frac{\partial \boldsymbol{\xi}}{\partial \mathbf{x}} \right)^\top \mathbf{K} \left( \frac{\partial \boldsymbol{\xi}}{\partial \mathbf{x}} \right). \quad (4)$$

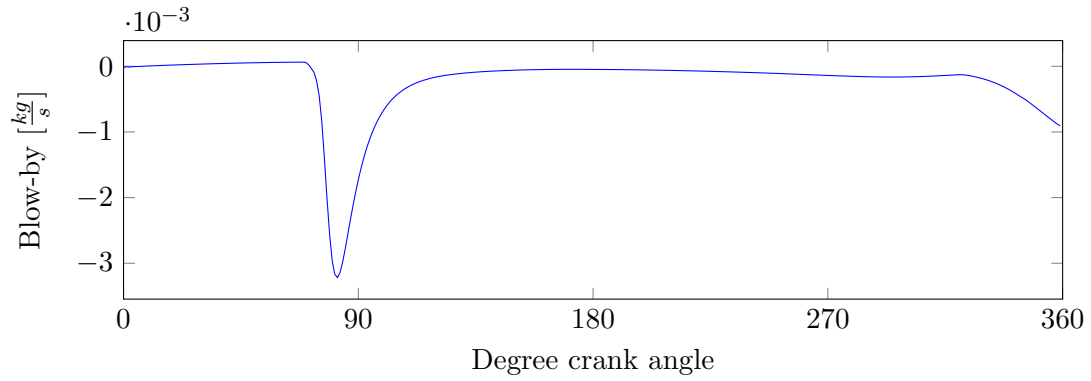
Specific for the discretization with space-time finite elements is the fifth term: It is used to weakly enforce the continuity of the solution between the current time slab  $(\mathbf{Y})_n^+$  and the previous one  $(\mathbf{Y})_n^-$  on the time level  $\Omega_n$ .

## 2 Flow Inside Piston Ring Pack

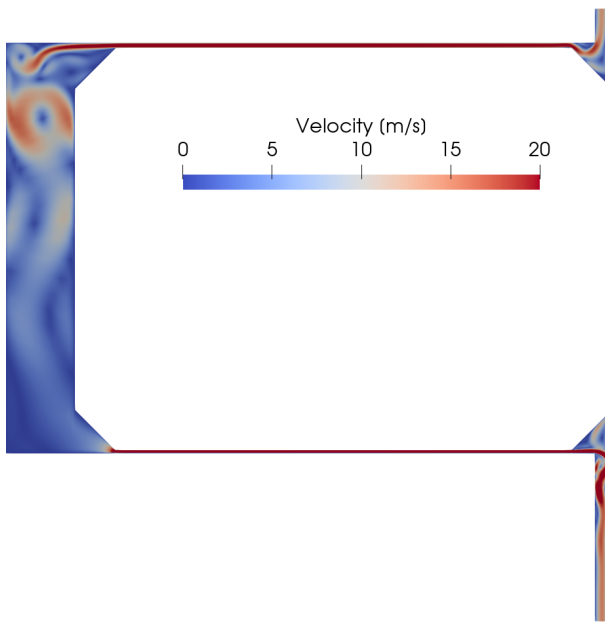
### 2.1 Model formulation

To apply this methodology to the flow in the piston ring pack, we formulate the following model: As the top ring is exposed to the largest pressure gradient, we focus on the flow around this ring to examine the sealing properties of the piston ring pack. For the transient computation (in Section 2.2), we select a two-dimensional cut through the top ring along the piston axis and discretize it with space-time finite elements. This results in a grid with 146561 degrees of freedom. The suction effect of the ring end gap is investigated with a three-dimensional computational domain including half of the ring end gap and  $12^\circ$  of the top ring in circumferential direction (see Section 2.3). The corresponding discretization has 3.4 million degrees of freedom.

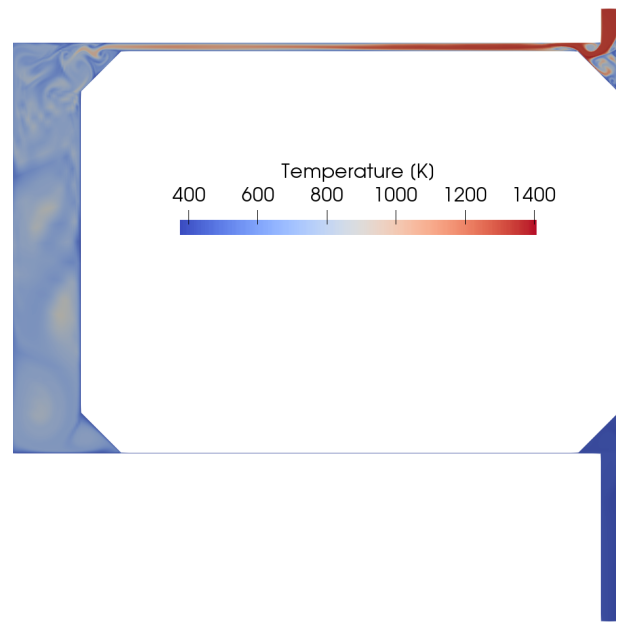
The flow in the piston ring pack is modeled as single compressible gas phase. We select a piston-fixed coordinate system and prescribe the relative velocity of piston and liner on the respective domain boundary. At the upper domain boundary pressure and temperature of the combustion chamber are prescribed; on the lower boundary the conditions of the crank case are applied. On the solid walls of the piston, liner, and ring, no slip conditions and temperatures according to [1] are prescribed. The relative motion of the piston ring inside the groove is prescribed based on data of our industry partner. The resulting mesh motion is handled with the deforming-spatial-domain/stabilized space-time (DSD/SST) procedure [4].



(a) Temporal evolution of blow-by past top ring



(b) Velocity field at 87.4° crank angle



(c) Temperature at 360° crank angle

Figure 2. Results of the transient two-dimensional computation.

## 2.2 Transient working cycle behavior

A central result of the transient computation is the evolution of the blow-by displayed in Figure 2a. As long as the ring is tightly aligned with the upper groove edge (until 70° crank angle), it seals the gas in the combustion chamber against the moderate pressure gradient of ca. 0.5 bar towards the crank case. During the edge change of the piston ring, the gap between ring and groove opens and allows for blow-by. The spatially resolved velocity field around the ring can be seen in Figure 2b. After the edge change, the ring is tightly aligned with the groove's lower edge and again seals the combustion chamber. Only as the combustion chamber pressure and temperature rise towards the combustion at 360° crank angle, the blow-by increases again. Figure 2c shows the gas temperature around the top ring at 360° crank angle.

## 2.3 Suction effect of the ring end gap

Figure 3 indicates that the suction effect of the ring end gap is limited to the first third of the computational domain, which corresponds to 4° in circumferential direction around the piston perimeter, at the beginning of the engine working cycle at 0.24° crank angle. High flow velocities of more than 200  $\frac{m}{s}$  are only present in the ring end gap. The three-dimensional simulation has to be continued to investigate the influence of the ring end gap for further states of the working cycle, in particular for higher pressure gradients.

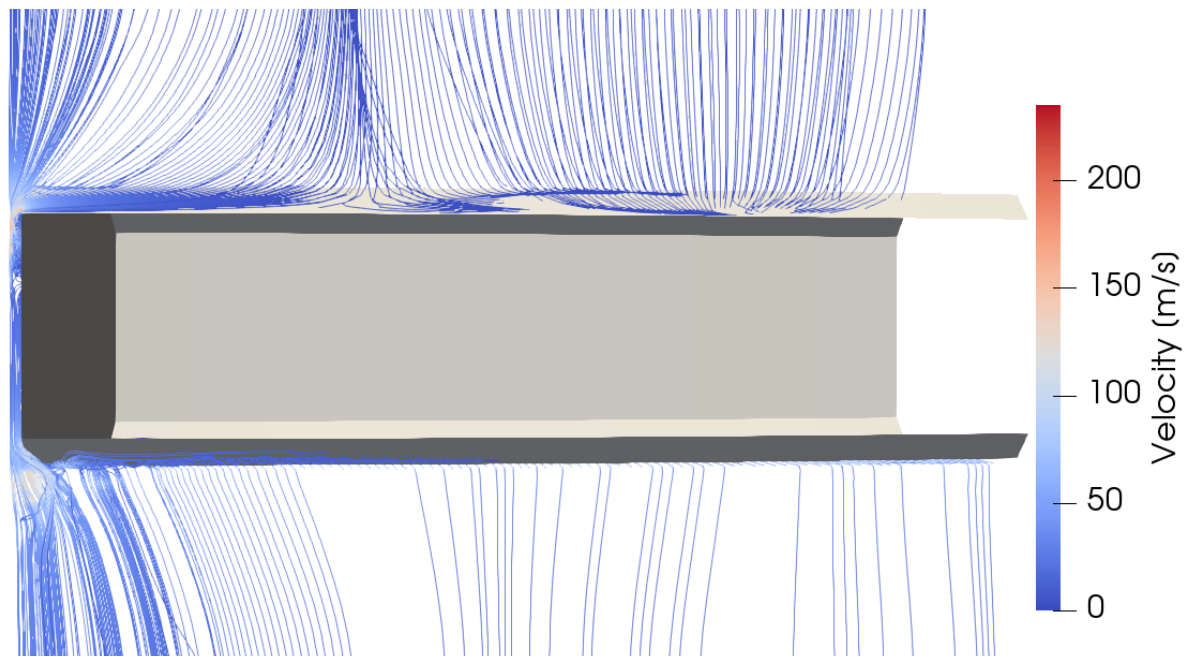


**Figure 3.** Three-dimensional flow field around top ring at  $0.24^\circ$  crank angle

## Conclusions

In this contribution, we extended the stabilized formulation for compressible flows of [5] for the discretization with space-time finite elements. The adjusted formulation is used successfully to analyze the internal compressible flows inside the piston ring pack of an internal combustion engine.

## Acknowledgements

This work was supported by the German Federal Ministry for Economic Affairs and Energy through the Central Innovation Programme for SMEs in the cooperation project "Simulationstechnik Kolben-Kolbenring-Zylinder". Computing resources were provided by RWTH Aachen University IT Center and Jülich Aachen Research Alliance (JARA).

## References

- [1] P. Lyubarsky and D. Bartel. 2d cfd-model of the piston assembly in a diesel engine for the analysis of piston ring dynamics, mass transport and friction. *Tribology International*, 104:352–368, 2016.
- [2] A. Oliva and S. Held. Numerical multiphase simulation and validation of the flow in the piston ring pack of an internal combustion engine. *Tribology International*, 101:98–109, 2016.
- [3] L. Pauli and M. Behr. On stabilized space-time fem for anisotropic meshes: Incompressible navier–stokes equations and applications to blood flow in medical devices. *International Journal for Numerical Methods in Fluids*, 85:189–209, 2017.
- [4] T. Tezduyar, M. Behr, and J. Liou. A new strategy for finite element computations involving moving boundaries and interfaces—the dsd/st procedure: I. the concept and the preliminary numerical tests. *Computer Methods in Applied Mechanics and Engineering*, 94(3):339–351, 1992.
- [5] F. Xu, G. Moutsanidis, D. Kamensky, M.-C. Hsu, M. Murugan, A. Ghoshal, and Y. Bazilevs. Compressible flows on moving domains: Stabilized methods, weakly enforced essential boundary conditions, sliding interfaces, and application to gas-turbine modeling. <http://dx.doi.org/10.1016/j.compfluid.2017.02.006>, 2017.